Application of unified equivalent frame method to two-way slab structures with beams

Seung-Ho Choi[1a], Deuck Hang Lee[2b], Jae-Yuel Oh[1c], Hae-Chang Cho[1d],
Jae-Yeon Lee[3e] and Kang Su Kim[*1]

[1]*Department of Architectural Engineering, University of Seoul, 163 Siripdaero, Dongdaemun-gu, Seoul,02504, Korea*
[2]*Department of Civil Engineering, Nazarbayev University, Kabanbay Batyr Ave 53, Astana 010000, Kazakhstan*
[3]*Division of Architecture, Mokwon University, 88 Doanbuk-ro, Seo-gu, Daejeon, 35349, Korea*

Abstract. The current design codes present an equivalent frame method (EFM) for the analysis and design of two-way slab structures. However, since the EFM was developed to be suitable for two-way slab structures subjected to gravity loads only, it brings many problems in its application to the analysis of two-way slabs to which gravity and lateral loads are applied simultaneously. Therefore, authors proposed the unified equivalent frame method (UEFM) that can analyze the structural behavior of flat-plate slab systems subjected to gravity and lateral loads in their previous studies. In this study, the UEFM was modified to be applicable to the two-way slab system with beams. In addition, the accuracy of the proposed UEFM was then examined by comparing it to the lateral behaviors of the two-way slab specimens.

Keywords: two-way slab; lateral load; gravity load; equivalent frame method; transverse beam; parallel beam

1. Introduction

The flat-plate slab system without beams has a variety of advantages, such as a simplified form work and efficient reduction in floor height (Raquib and Fatema 2017, Kim and Kang 2017, Youssef *et al.* 2014, Almeida *et al.* 2016, Ricker *et al.* 2017), but poses disadvantages in that the shear performance around the column can be insufficient when large loads are applied, or it is difficult to control deflection when the span length is long. (Alexander and Simmonds 1987, MacGregor and Wight 2006, Widianto *et al.* 2009, Gardner 2011) For these reasons, the two-way slab structure with transverse and parallel beams shown in Fig. 1 has widely been applied until recently. The equivalent frame method (EFM) is known as a representative analysis method for the two-way slab system, and the current design codes permit the application of EFM to the lateral behavior analysis of the two-way slab system. However, since the existing EFM has been developed to be suitable for a two-
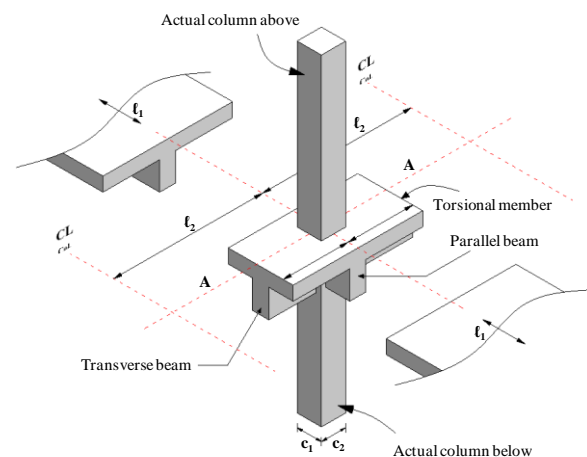

Fig. 1 Two-way slab system with transverse and parallel beams

way slab system subjected to gravity loads only, its applicability to a system subjected to lateral loads seems to be uncertain, and therefore various analysis models have been proposed to address this issue. (Hwang and Moehle 2000, Park *et al.* 2009, Kim *et al.* 2014, Choi *et al.* 2014, Choi *et al.* 2017) The EFM specified in ACI 318 prescribes that the torsional constant should be calculated considering the cross-sectional area of the transverse beam for the two-way slab with a transverse beam. It also provides that, in the presence of a parallel beam, the stiffness of the attached torsional member (K_t) should be increased by the ratio of the moment of inertia of the slab including the composite parallel beam (I_{sb}) to the moment of inertia of the slab (I_s), as suggested by Corley and Jirsa (1970). However, this

---

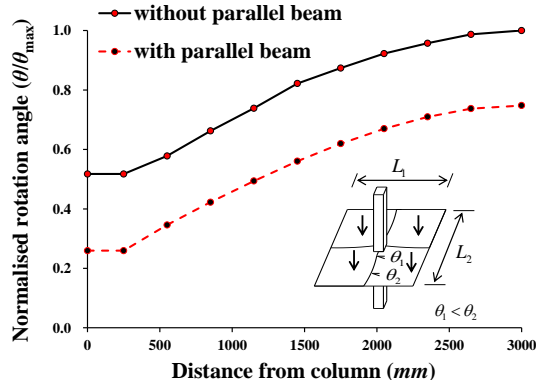∗Corresponding author, Professor
 E-mail: kangkim@uos.ac.kr
[a]Ph.D. Candidate
 E-mail: ssarmilmil@uos.ac.kr
[b]Assistant Professor
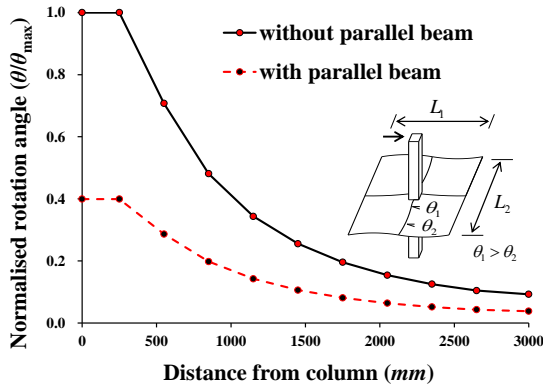 E-mail: deuckhang.lee@nu.edu.kz
[c]Ph.D.
 E-mail: hahappyppy@naver.com
[d]Post-Doctoral Fellow
 E-mail: chang41@uos.ac.kr
[e]Professor
 E-mail: jylee@mu.ac.kr

(a) Distribution of rotational angle due to gravity loads

(b) Distribution of rotational angle due to lateral loads

Fig. 2 Effect of parallel beam on rotation angle distributions of torsional elements attached (c=500 mm, L_1=L_2= 6000 mm, beam size=500 mm×500 mm)

method does not reflect changes in the torsional moment distribution due to the presence of parallel beams. Figs. 2(a) and (b) show the finite-element analysis results of two-way slab-column connection subassemblies under gravity and lateral loads, respectively. As shown in Fig. 2(a), the torsional rotation angle around the surface of a column is smaller than that in the center of a slab because of the inflexibility of the column when only the gravity loads are applied. In addition, when the parallel beam is present, the rotation angle of the torsional member is smaller than that of cases in which there is no parallel beam. Meanwhile, when the lateral loads are applied, the rotation of the column is preceded by the lateral loads, and a larger torsional rotation occurs in the slab near the surface of the column than in the center of the slab, as shown in Fig. 2(b) (Park *et al*. 2009). In addition, as in the case where the gravity loads are applied, the torsional rotation is smaller when the parallel beam is present than when there is no parallel beam, even when the lateral loads are applied.

As explained, the torsional member shows very different rotational behaviors when either the gravity loads or the lateral loads are applied, and the magnitude of the torsional rotation depends on the presence or absence of the parallel beam. Therefore, in this study, the authors have modified the unified equivalent frame method (UEFM) developed in their previous research to make it suitable for the analysis of flat-plate systems with transverse and parallel beams subjected to gravity and lateral loads.
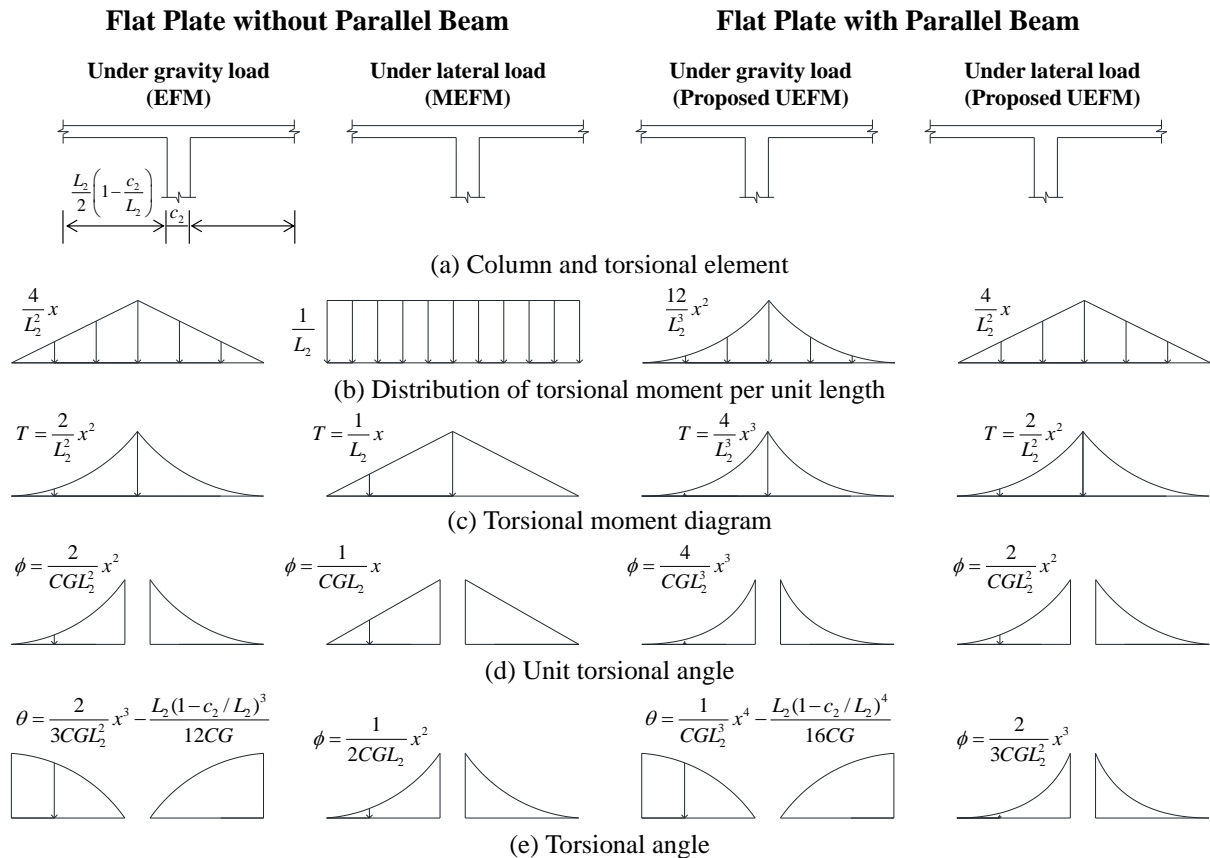

Fig. 3 Rotational stiffness of attached torsional members with and without parallel beams

2. Review of previous research (Unified equivalent frame method (UEFM))

As shown in Figs. 3(a) and (b), the equivalent frame method (EFM) assumes a triangular distribution of torsional moment per unit length when the gravity loads are applied, whereas the modified equivalent frame method (MEFM) assumes that the torsional moments per unit length are uniformly distributed when the lateral loads are applied. In ACI 318-14 and the MEFM, the stiffness of a torsional member (K_t) is presented, respectively, as follows

$$\text{ACI 318-14} \qquad K_t = \frac{9CE_c}{L_2\left(1 - c_2/L_2\right)^3} \qquad (1a)$$

$$\text{MEFM (Park \textit{et al.} 2009)} \quad K_t = \frac{6CE_c}{L_2\left(1 - c_2/L_2\right)^2} \qquad (1b)$$

where C is the torsional constant, E is the modulus of elasticity of concrete, c_2 is the slab width perpendicular to the design strip, and L_2 is the column width in the perpendicular to the design direction.

However, since the gravity and lateral loads are applied simultaneously in the actual structure, the torsional moment distribution takes a complex shape according to the combinations of the loads.

The stiffness of the torsional member is affected by the relative magnitude of the gravity and lateral loads. In the UEFM proposed in the authors' previous research, as shown in Fig. 4, the stiffness of the torsional member was presented by introducing a load-ratio factor (λ_c) that is the ratio of the torsional moment caused by lateral loads to the torsional moment caused by gravity loads, and the stiffness of the torsional member ($K_{t,\lambda c}$) was suggested to be

$$K_{t,\lambda c} = \frac{18CE\left(1 + \lambda_c\right)}{L_2\alpha^2\left(2\alpha + 3\lambda_c\right)} \qquad (2)$$

where α is $1 - c_2/L_2$. If only the gravity loads are applied, the load-ratio factor becomes zero, and then the stiffness of the torsional member is consistent with the stiffness of the torsional member as calculated by means of the equivalent column concept of the EFM. In addition, if the lateral loads become too large, the load-ratio factor will also become large when the stiffness of the torsional member converges to that of the torsional member presented in the modified equivalent frame method (Park *et al.* 2009) based on the equivalent slab concept.

3. Proposed model

3.1 Effect of a transverse beam

As shown in Fig. 5, ACI 318 considers the effects of transverse beams when calculating the torsional constant (C) in the two-way slab with a transverse beam. If there is no transverse beam, as shown in Fig. 5(a), the torsional constant (C) is calculated under the assumption that the torsional member is a rectangle with the height of the slab (h_f) and column width in the loading direction (c_1) as both
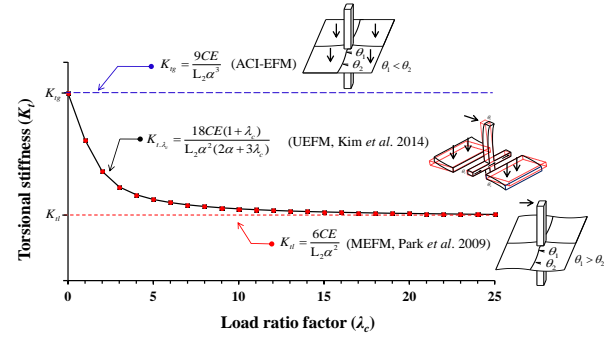

Fig. 4 Effect of load ratio factor on stiffness of torsional member

(a) Torsional section without transverse beam

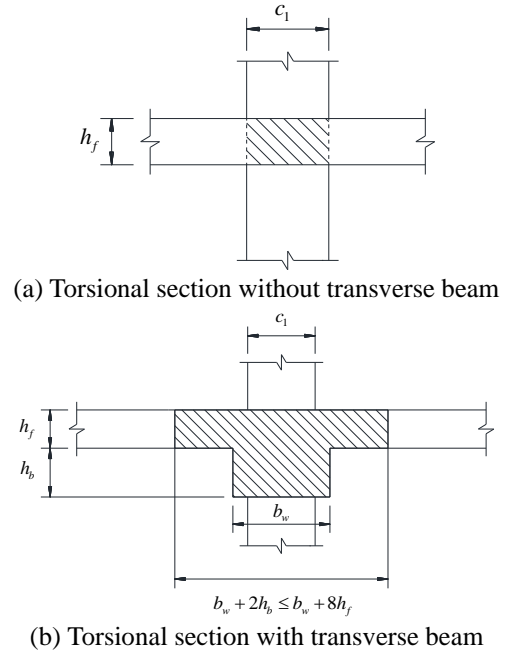(b) Torsional section with transverse beam

Fig. 5 Effective section for calculation of torsional constant (C)

sides. On the other hand, if a transverse beam is present, the torsional constant (C) is calculated by considering the torsional member to be a T-shaped section that includes the portion of the slab extended to both sides of the transverse beam, as long as the height (h_b) of the transverse beam, when the width extended by the transverse beam is less than four times the slab thickness; i.e., $h_b < 4h_f$. In the presence of a transverse beam, this method can very simply reflect the stiffness of the torsional member in the analysis, and therefore the same method is applied in this study.

3.2 Effect of a parallel beam

In the EFM presented in ACI 318, the stiffness of the torsional member in the two-way slab with a parallel beam is multiplied by the ratio of the moment of inertia of the slab and parallel beam (I_{sb}) to the moment of inertial of the slab (I_s). The stiffness of the torsional member, which is increased by the parallel beam, is calculated as

$$\frac{1}{K_{ec}} = \frac{1}{\sum K_c} + \frac{1}{K_{tg}\left(I_{sb}/I_s\right)} \qquad (3)$$

where K_c is the flexural stiffness of the column, K_{tg} is the stiffness of the torsional member in a two-way slab system subjected to gravity loads, and K_{ec} is the stiffness of the equivalent column. This method was proposed by Corley and Jirsa (1970) and can reflect the effects of the parallel beam in a very simple way. As shown in Fig. 3, the EFM assumes that the distribution of the torsional member of the two-way slab structure without a parallel beam is triangular. However, when the parallel beam is placed, the stiffness of the column to which the parallel beam is attached increases, and the distribution and magnitude of torsional moment are changed. Therefore, in order to reflect the effect of the parallel beam, the distributions of torsional moments per unit length under gravity and lateral loads were modified to be a quadratic curve and a triangular distribution, respectively, instead of the existing triangular and uniform distributions. Under gravity and lateral loads, if the torsional moment when the gravity loads act on the two-way slab with the parallel beam is assumed to be unity (i.e., 1.0), as shown in Fig. 6, the relative magnitude of the torsional moment induced by the lateral loads can be represented by using the load-ratio factor in the two-way slab with a parallel beam (λ_b). That is, λ_b can be defined as

$$\lambda_b = \frac{T_l}{T_g} \tag{4}$$

where T_l is the moment in torsional members induced by lateral loads, and T_g is the moment in torsional members induced by gravity loads. It should be noted that the ratio of lateral to gravity loads can be changed, and so does the λ_b.

Accordingly, the maximum torsional angles ($\theta_{g,\max}$ and $\theta_{l,\max}$) caused by gravity and lateral loads in the two-way slab with a parallel beam are represented by equations 4 and 5, respectively.

$$\theta_{g,\max} = \frac{L_2(1-c_2/L_2)^4}{16CG} \tag{5}$$

$$\theta_{l,\max} = \frac{L_2(1-c_2/L_2)^3}{12CG}\lambda_b \tag{6}$$

where G is the shear modulus of concrete. If the average rotation angle of the torsional member ($\theta_{g,ave}$ and $\theta_{l,ave}$) is assumed to be 1/3 of the maximum torsional rotation angle ($\theta_{g,\max}$ and $\theta_{l,\max}$), and the shear modulus of concrete (G) to be half of the elastic modulus ($E/2$), respectively, and the Poisson's effect is neglected, the average torsional angles ($\theta_{g,ave}$ and $\theta_{l,ave}$) in the two-way slab with a parallel beam, which are induced by gravity and lateral loads, can be calculated by Eqs. (7) and (8), respectively.

$$\theta_{g,ave} = \frac{L_2(1-c_2/L_2)^4}{24CE} \tag{7}$$

$$\theta_{l,ave} = \frac{L_2(1-c_2/L_2)^3}{18CE}\lambda_b \tag{8}$$

The total torsional moment acting on the equivalent frame becomes $1+\lambda_b$, and the rotation angle of the torsional members in the two-way system subjected to gravity and lateral loads (θ_{tot}) can be calculated as the sum of the rotational contribution of the torsional members to the equivalent column ($\theta_{g,ave}$) and the rotational contribution of the torsional members to the equivalent slab ($\theta_{l,ave}$). As shown in Fig. 6, the moment distribution and the rotation angle are symmetric about the center of the column, and therefore if only the left half is considered, the rotation angle and total moment of the torsional member in the two-way slab system subjected to gravity and lateral loads (θ_{tot} and T_{tot}) are

$$\theta_{tot} = \frac{L_2\alpha^3(3\alpha+4\lambda_b)}{72CE} \tag{9}$$

$$T_{tot} = \frac{1+\lambda_b}{2} \tag{10}$$

where α can be taken to be $1-c_2/L_2$. Thus, the effective stiffness of the torsional members in the two-way slab system with parallel beams subjected to gravity and lateral loads (K_{t,λ_b}) can be derived by

$$K_{t,\lambda_b} = \sum\frac{T_{tot}}{\theta_{tot}} = \sum\frac{36CE(1+\lambda_b)}{L_2\alpha^3(3\alpha+4\lambda_b)} \tag{11}$$
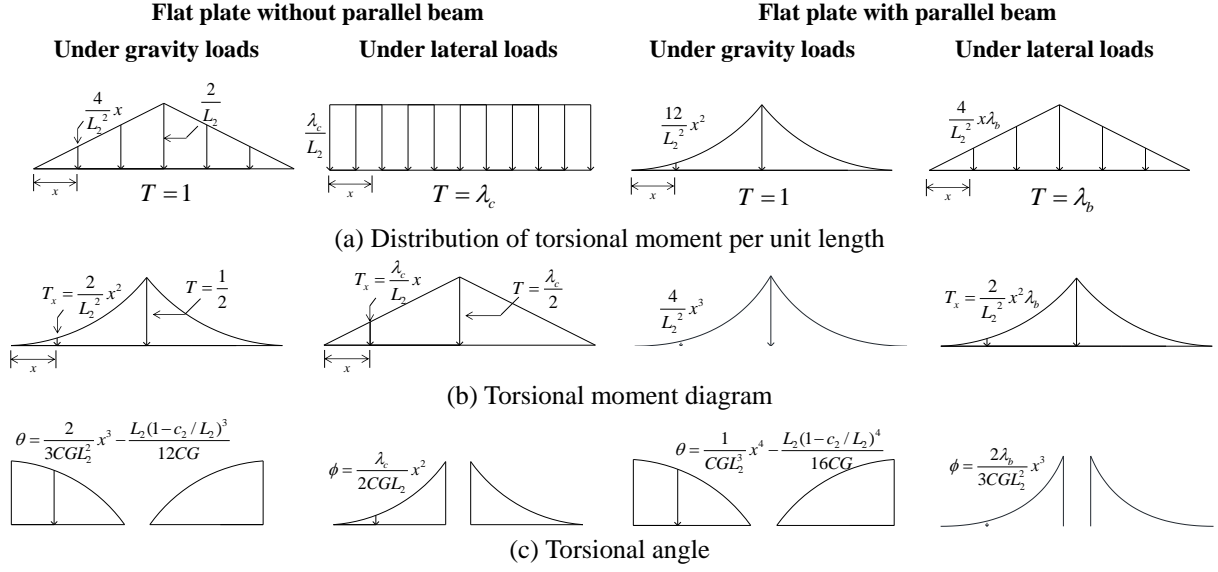
Therefore, if only the load-ratio factor in the two-way slab with a parallel beam (λ_b) is calculated, the effective stiffness of the torsional member in the two-way slab system with parallel beams subjected to gravity and lateral loads (K_{t,λ_b}) can be found. λ_b is the ratio of the torsional moment caused by the gravity and lateral loads, or T_l/T_g. With respect to T_g, the concept of the equivalent column is applied, and the flexural moment acting on the slab by the gravity loads is distributed to the column and torsional member. With respect to T_l, the equivalent slab concept is applied, and the unbalanced moment acting on the slab-column connection by the lateral loads is distributed to the slab and torsional member. That is, T_g and T_l can be calculated by Eqs. (12) and (13), respectively.

$$T_g = M_s\frac{K_{tg}}{K_{tg}+\sum_{i=1}^{n}K_{ci}} \tag{12}$$

$$T_l = M_{ub}\frac{K_{tl}}{K_{tl}+\sum_{i=1}^{n}K_{si}} \tag{13}$$

where M_s is the flexural moment at the end of the slab by gravity loads (i.e., the fixed-end moment of the slab member), and M_{ub} is the unbalanced moment at the slab-column connection by lateral loads, which is identical to the sum of bending moments in the upper and the lower columns developed at joint ($M_{cb}+M_{ct}$).

Fig. 7 represents the torsional stiffness of the two-way slab with and without parallel beams with respect to the load-ratio factor (λ_c and λ_b). As compared with the two-way slab without a parallel beam, the stiffness of the torsional member is greatly increased when there is a parallel beam. In the presence of a parallel beam, the stiffness of the torsional member increases from $9CE/L_2\alpha^3$ to $12CE/L_2\alpha^4$

Flat plate without parallel beam

Under gravity loads	Under lateral loads

Flat plate with parallel beam

Under gravity loads	Under lateral loads

(a) Distribution of torsional moment per unit length

(b) Torsional moment diagram

(c) Torsional angle

Fig. 6 Load ratio factor (λ_b) in the proposed UEFM

Fig. 7 Comparison of stiffness of torsional members with and without parallel beam

when only the gravity loads are applied, and increases from $6CE/L_2\alpha^3$ to $9CE/L_2\alpha^3$ when the lateral loads are dominant. Since the rotation angle of the torsional member ($\theta_{t,gravity}$) by gravity loads contributes to the rotation of the equivalent column (θ_{ec}), and the rotation angle of the torsional member ($\theta_{t,lateral}$) by lateral loads contributes to the rotation of the equivalent slab (θ_{es}), these rotation angles and those of the column, slab, and torsional members (θ_c, θ_s and θ_t) can be represented as the following relations.

$$\theta_t = \theta_{t,gravity} + \theta_{lateral} \tag{14a}$$

$$\theta_{ec} = \theta_{t,gravity} + \theta_c \tag{14b}$$

$$\theta_{es} = \theta_{t,lateral} + \theta_s \tag{14c}$$

Therefore, the flexibility relationship between the equivalent column and the equivalent slab can be represented by Eqs. (15a) and (15b), respectively.

$$\frac{1}{K_{ec}} = \theta_{t,gravity} + \theta_c = \frac{\sum K_c}{\sum K_c + \sum K_s} \frac{1}{K_{t,\lambda_b}} + \frac{1}{\sum K_c} \tag{15a}$$

$$\frac{1}{K_{es}} = \theta_{t,lateral} + \theta_s = \frac{\sum K_s}{\sum K_c + \sum K_s} \frac{1}{K_{t,\lambda_b}} + \frac{1}{\sum K_s} \tag{15b}$$

In the two-way slab, the beam placed along the centerline of the column should have no problem transferring the loads acting on the affected floor area to the column (Leet and Bernal 1997). Therefore, the current design codes define the beam-to-slab stiffness ratio (α_1) of slabs with and without beams as

$$\alpha_1 = \frac{4E_{cb}I_b/l}{4E_{cs}I_s/l} = \frac{E_{cb}I_b}{E_{cs}I_s} \tag{16}$$

In addition, it provides different moment distribution ratios depending on the value of $\alpha_1 L_2/L_1$, as based on the
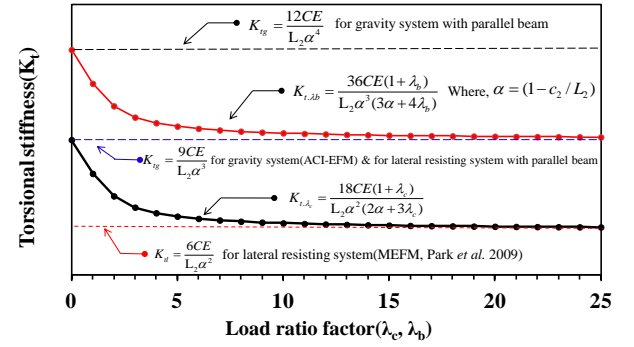
research results of MacGregor and Wight (2006). In this study, the effect of the parallel beam is reflected only when the size of the parallel beam can satisfy $\alpha_2 L_2/L_1 > 1.0$ (i.e., when the beam is big enough).

4. Verification of proposed method

4.1 Two-way slab system with transverse beams

Fig. 8(a) shows the dimension details of the two-story two-way slab with the transverse beam specimen by Moehle and Diebold (1984). The length and height of the test specimen were 5.49 m and 2.22 m, respectively. The transverse beams are located on the first story and the second story of the exterior columns. As shown in Fig. 8(b), a finite- element analysis was performed using ABAQUS, a commercial finite-element analysis program. Since the upper and lower sides, as well as the left and right sides, are symmetric when viewed in a plane, only a quarter of the test specimen was modeled, and an eight-node hexahedral element (C3D8R) among 3D solid elements was used for the slab and column. To simplify the modeling, a two-node linear 3D truss element (T3D2) was used to model the steel
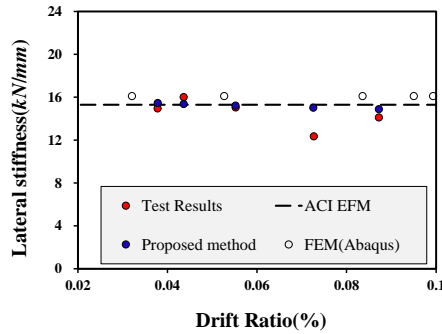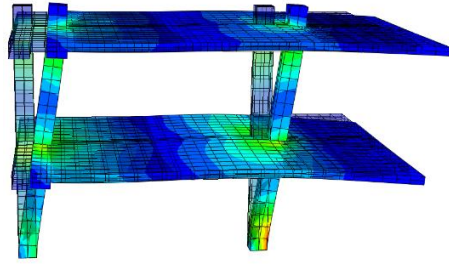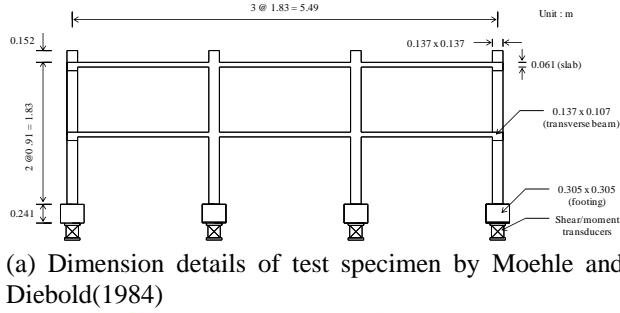
(a) Dimension details of test specimen by Moehle and Diebold(1984)

(b) 3D FE analysis model of test specimen

(c) Comparison of test and analysis results

Fig. 8 Verification of proposed method for two-way slab structure with transverse beams

(a) Dimension details of example structure

(b) Effect of beam size

(c) Effect of column size

Fig. 9 Verification of proposed method for two-way slab structure with parallel beams

reinforcement. The material test results reported in the paper of Moehle and Diebold (1984) were used for the properties of materials. The concrete-damaged plasticity model (Lubliner *et al*. 1989, Lee and Fenves 1998, Kmiecik and Kaminski 2011) was used to reflect the nonlinearity of concrete on the compression side as well as the tension softening. The elasto-perfectly plastic model was used for the material models of the steel reinforcement. The reinforcement placed in concrete was modeled by means of the embedded region option, assuming a perfect bond between the reinforcement and the concrete. The lower end of each column was constrained against displacement in all directions, and the rotation was unconstrained in order to simulate the same boundary conditions as the experimental conditions. Fig. 8(c) compares the test results and analysis results obtained using ACI-EFM, the proposed model, and the detailed finite-element analysis, and it shows drift ratios up to 0.1% before the stiffness degrades because of the cracks in the columns and slabs. The results analyzed using ACI-EFM, the proposed model, and the detailed finite-element analysis show lateral stiffness to very similar that of the test results, because the frame behaves dominantly by the effect of gravity loads when the lateral loads are small (i.e., the drift ratio is small).
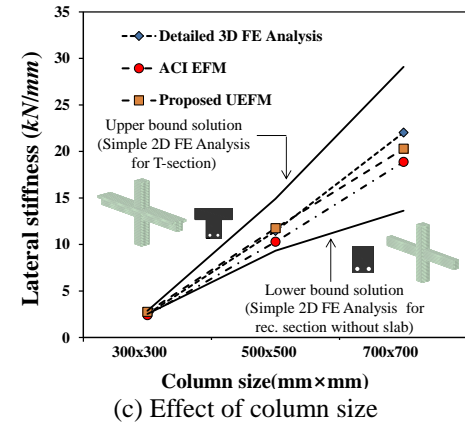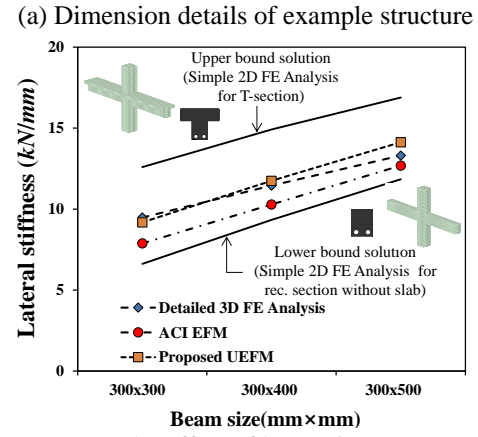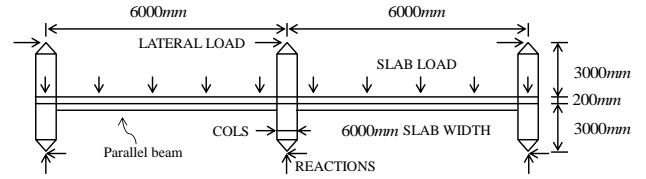
4.2 Two-way slab system with parallel beams

Since the test results of the two-way slab with parallel beams cannot be found from the existing literature, an example structure subjected to gravity and lateral loads is introduced as shown in Fig. 9(a). The example structure is a two-span structure with a slab of 6,000 mm×6,000 mm×200 mm; the length of the top and bottom columns is 3,000 mm. The modulus of the elasticity of the concrete is 28,000 N/mm^2, and the amount of gravity loads applied per unit area is 5 kN/m^2. As mentioned above, in the proposed model, the effective stiffness (K_{t,λ_b}) of the torsional member is calculated by considering the effect of the parallel beam and the combination of gravity and lateral loads.

Fig. 9(b) shows the analysis results obtained by changing the height of the parallel beam to 300 mm, 400 mm, and 500 mm, with the size of the column fixed to 500 mm×500 mm, where the analysis result displays lateral stiffness at about a 0.1% drift ratio. In the graph, the upper bound solution is a result calculated by means of a two-dimensional finite-element analysis model under the

(a) Dimension details of example structure modified from the test specimen by Moehle and Diebold (1984)

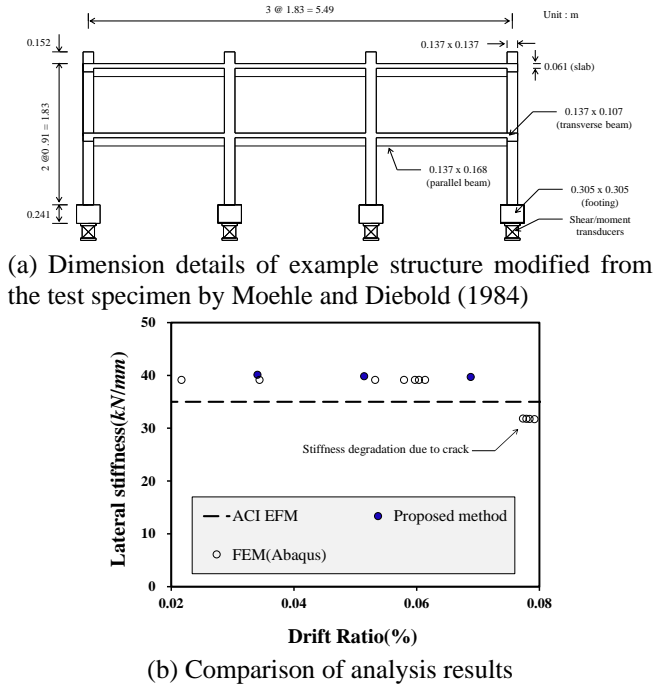(b) Comparison of analysis results

Fig. 10 Verification of proposed method for two-way slab structure with transverse and parallel beams

assumption that the slab and the parallel beam are T-beams.

On the other hand, the lower bound solution is a result analyzed by assuming the Rahmen structure consisting of a rectangular beam and a column, ignoring the influence of the slab, and thus it exhibits lower lateral stiffness than in other analyses. The detailed 3D FE analysis is the result of a 3D finite-element analysis conducted using ABAQUS, and it can be confirmed that the stiffness of the frame is between the stiffness value of the upper bound and that of the lower bound. The detailed 3D FE analysis results showed that the lateral stiffness of the frame increases with the increasing height of the parallel beam, and the proposed model evaluated this tendency relatively accurately.

On the other hand, the EFM provided relatively low lateral stiffness, which suggests that the EFM cannot reflect the change in magnitude and distribution of torsional moment caused by the parallel beam, as shown in Fig. 6. Fig. 9(c) shows the analysis results obtained by changing the column size with the size of the parallel beam fixed to 300 mm×400 mm. As in the results of the analysis using the beam size as a variable, the EFM also provided a lateral stiffness lower than that obtained by the detailed 3D FE analysis in the results of analysis using the column size as a variable. On the other hand, the lateral stiffness calculated by the proposed model was in good agreement with the detailed 3D FE analysis results.

4.3 Two-way slab system with transverse and parallel beams

As mentioned earlier, the analysis results of the test specimen by Moehle and Diebold (1984) shown in Fig. 8 indicate that the accuracy of the detailed 3D FE analysis has been sufficiently verified. Therefore, in this study, a parallel

beam with a section of 138 mm×168 mm was placed on the entire span of the test specimen of Moehle and Diebold (1984), as shown in Fig. 10(a), and the result obtained by the detailed 3D FE analysis was regarded as an exact solution. Fig. 10(b) compares the analysis results obtained using the proposed model and EFM and those obtained using the detailed 3D FE analysis. The analysis result obtained using the EFM was found to underestimate the initial lateral stiffness of the frame with respect to the two-way slab structure with transverse and parallel beams. The results shown in Fig. 8(c) indicate that the EFM predicted the initial lateral behavior of the frame without a parallel beam relatively accurately. However, as shown in Fig. 9 and Fig. 10, the EFM underestimated the lateral stiffness of the frame because it failed to reflect the distribution and magnitude of torsional moment when there is a parallel beam. On the other hand, the analysis results obtained from the UEFM proposed in this study showed a initial stiffness almost similar to that of the FEM analysis. In the FEM, cracks occurred at the drift ratio of 0.08%, and the stiffness decreased. However, it was found that the proposed model cannot accurately evaluate the lateral stiffness after cracking, because it cannot consider the stiffness degradation resulting from the cracks and the nonlinear behavior of materials. Therefore, there is a need to apply an appropriate stiffness-reduction factor to more accurately simulate the lateral stiffness degradation resulting from cracking in the two-way slab structure with transverse and parallel beams.

5. Conclusions

This study proposed the unified equivalent frame method (UEFM) as being suitable for the analysis of the lateral behaviors of the two-way slab structure with transverse and parallel beams subjected to combined gravity and lateral loads. The following conclusions were obtained from the results of this study.

1. The EFM presented in ACI318-14 has been developed to be suitable for a two-way slab system subjected to gravity loads only, and its applicability to a system subjected to lateral loads could be uncertain.

2. In the proposed model, the effect of the transverse beam was reflected in the torsional constant, and the proposed model was verified using the test results of the two-way slab structure with a transverse beam by Moehle and Diebold (1984).

3. The distribution and magnitude of torsional moment are changed in the presence of a parallel beam as compared to the two-way slab structure without a parallel beam, and the effective stiffness of the torsional member in the two-way slab system with a parallel beam subjected to gravity and lateral loads ($K_{t,\lambda b}$) that can reflect this was proposed in this study.

4. The structural behavior of the two-way slab structure with parallel beams added to the test specimen of Moehle and Diebold (1984) was analyzed by means of finite-element analysis, the EFM, and the proposed model. The analysis revealed that the proposed model provides a highly accurate simulation of the initial

lateral stiffness of the structure.

Acknowledgments

References

ACI Committee 318 (2014), Building Code Requirements for Structural Concrete and Commentary (ACI 318-14), American Concrete Institute, Farmington Hills, MI.

Alexander, S.D.B. and Simmonds, S.H. (1987), "Ultimate strength of slab-column connections", *ACI Struct. J.*, **84**(3), 255-261.

Almeida, A.F.O., Inácio, M.M.G., Lúcio, V.J.G. and Ramos, A.P. (2016), "Punching behaviour of RC flat slabs under reversed horizontal cyclic loading", *Eng. Struct.*, **117**(1), 204-219.

Choi, S.H., Lee, D.H., Oh, J.Y., Kim, K.S., Lee, J.Y. and Lee, K.S. (2017), "Unified equivalent frame method for post-tensioned flat plat slab structures", *Comput. Concrete*, **20**(6), 663-670.

Choi, S.H., Lee, D.H., Oh, J.Y., Kim, K.S., Lee, J.Y. and Shin, M.S. (2014), "Unified equivalent frame method for flat plate slab structures under combined gravity and lateral loads-Part 2: verification", *Earthq. Struct.*, **7**(5), 735-751.

Corley, W.G. and Jirsa, J.O. (1970), "Equivalent frame analysis for slab design", *ACI J. Proc.*, **67**(11), 875-884.

Gardner, N.J. (2011), "Verification of punching shear provisions for reinforced concrete flat slabs", *ACI Struct. J.*, **108**(5), 572-580.

Kim, J.Y. and Kang, S.M. (2017), "Simulations of short- and long-term deflections of flat plates considering effects of construction sequences", *Struct. Eng. Mech.*, **62**(4), 477-485.

Kim, K.S., Choi, S.H., Ju, H.J., Lee, D.H., Lee, J.Y. and Shin, M.S. (2014), "Unified equivalent frame method for flat plate slab structures under combined gravity and lateral loads-Part 1: Derivation", *Earthq. Struct.*, **7**(5), 719-733.

Kmiecik, P. and Kaminski, M. (2011), "Modeling of reinforced concrete structures and composite structures with concrete strength degradation taken into consideration", *Arch. Civil Mech. Eng.*, **11**(3), 623-636

Lee, J.H. and Fenves, G.L. (1998), "Plastic-damage model for cyclic loading of concrete structures", *J. Eng. Mech.*, ASCE, **124**(8), 892-900.

Leet, K. and Bernal, D. (1997), *Reinforced Concrete Design*, 3th Edition, McGraw-Hill Co.

Lubliner, J., Oliver, J., Oller, S. and Oñate, E. (1989), "A plastic-damage model for concrete", *Int. J. Solid. Struct.*, **25**(3), 299-326.

MacGregor, J.G. and Wight, J.K. (2006), *Reinforced Concrete Mechanics and Design*, 4th Edition, Prentice-Hall Inc.

Moehle, J.P. and Diebold, J.W. (1984), "Experimental study of the seismic response of a two-story flat-plate structure", University of California, Berkeley, CA.

Park, Y.M., Han, S.W. and Kee, S.H. (2009), "A modified equivalent frame method for lateral load analysis", *Mag. Concrete Res.*, **61**(5), 359-370.

Raquib, A. and Fatema, T.Z. (2017), "Numerical study on effect of integrity reinforcement on punching shear of flat plate", *Comput. Concrete*, **20**(6), 731-738.

Ricker, M., Häusler, F. and Randl, N. (2017), "Punching strength of flat plates reinforced with UHPC and double-headed studs", *Eng. Struct.*, **136**(1), 345-354.

Widianto, B.O. and Jirsa, J.O. (2009), "Two-way shear strength of slab-column connections: Reexamination of ACI 318 provisions", *ACI Struct. J.*, **106**(2), 160-170.

Youssef, M.A., Meshaly, M.E. and Chowdhury, A.O. (2014), "Lateral stiffness of reinforced concrete interior flat plate connections", *Eng. Struct.*, **62-63**, 23-32.

CC